DOI: 10.1002/chem.201000980

A General pH-Responsive Supramolecular Nanovalve Based on Mesoporous Organosilica Hollow Nanospheres

Wanping Guo, Jing Wang, Sang-Joon Lee, Fuping Dong, Sung Soo Park, and Chang-Sik Ha*[a]

Recently, increasing research interest has focused on the construction of molecular devices for the controlled release of guest molecules.[1] Supramolecular chemistry is a powerful methodology for the construction of various molecular devices, such as molecular shuttles, molecular motors, and nanovalves.[2] A supramolecular nanovalve can be defined as an assembly of two or more molecular components designed to perform valvelike motions to entrap and release guest molecules within nanopores on demand. Such operational nanovalves generally include gatekeepers that are constructed from donor–acceptor pseudorotaxanes or bistable rotaxanes, and mesoporous nanocontainers that act as a supporting platform for the gatekeepers and a reservoir for the guest molecules.[3] The supramolecular nanovalve is able to be operated by external stimuli; including redox,[4] light,[5] enzyme,[6] competitive binding,[7] and pH activation.[8–11] Among these external stimuli, pH-responsive activation represents a very convenient and feasible method to offer specific control with perturbation of protons by readily available acids and bases because measurement and change of pH in solution is simple and swift. In a first proof-of-concept, Stoddart and co-workers reported the design and synthesis of a pH-responsive supramolecular nanovalve consisting of the macrocyclic polyether dibenzo[24]crown-8 (DB24C8)/dialkylammonium cation pseudorotaxane as the gatekeeper and MCM-41 silica as the mesoporous nanocontainer.[8] This supramolecular system, the components of which, could be made to dissociate upon deprotonating the dialkylammonium thread by the addition of a base was held together by hydrogen bonding and operated in organic solvent CH_2Cl_2. Later, the same authors developed another pH-switchable nanovalve that operated within an aqueous acidic environment, using ion–dipole interaction between the hexameric macrocyclic cucurbit[6]uril (CB[6]) and bisalkylammonium cations.[9] At the same time, Kim and co-workers also demonstrated a new pH-responsive supramolecular nanovalve based on the hydrophobic-effect interaction between α- or γ-cyclodextrin (CD) and polyethyleneimine (PEI).[10] At pH 11, the mesopores were filled with guest molecules and blocked by the CD/PEI pseudorotaxane. Whereas at pH 5.5, the guest molecules were released from the mesopores by dethreading α- or γ-CD from the PEI chain due to amine protonation. The most recent example was involved in the formation of a supramolecular pseudorotaxane between α-CD and anilinoalkane held together by van der Waals forces and the hydrophobic-effect interaction.[11] At neutral pH, the α-CD/anilinoalkane pseudorotaxane blocked the departure of guest molecules. Upon protonating the nitrogen atoms in acidic media, the hydrophobic-effect interaction decreased and the α-CD was dissociated, allowing the entrapped guest molecules to escape. However, from the viewpoint of practical applications, such as controlled release of drugs and proteins, a smart nanovalve system not only employs biocompatible components, but also operates under flexible physiological conditions. In particular, to develop a general nanovalve that is able to operate in acidic, neutral, and basic aqueous media remains a challenge.

Until now, to the best of our knowledge, mesoporous silica-based nanoparticles have become an exclusive candidate as the nanocontainers of supramolecular nanovalves, since there are no reports on the employment of other kinds of mesoporous nanocontainers. Nevertheless, mesoporous silica materials such as MCM-41 are, in fact, not hydrothermally stable even in neutral aqueous media, let alone in acidic or basic media.[12] Compared with mesoporous silicas, periodic mesoporous organosilicas (PMO) are a new class of organic–inorganic hybrid materials that have comparable ordered pore structures and much higher hydrothermal stability.[13] Apparently, in addition to its hydrophobicity and bio-

[a] Dr. W. Guo, J. Wang, S.-J. Lee, F. Dong, Dr. S. S. Park, Prof. C.-S. Ha
Department of Polymer Science and Engineering
Pusan National University, Busan 609-735 (South Korea)
Fax: (+82) 51-514-4331
E-mail: csha@pusan.ac.kr

Supporting information for this article is available on the WWW under http://dx.doi.org/10.1002/chem.201000980.

compatibility,[14] mesoporous organosilica would be very attractive to be used as the nanocontainer in a nanovalve system.

Herein, we seek to develop a smart nanovalve system that integrates the advantages of existing pH-switchable nanovalves. We report the design of a general pH-responsive supramolecular nanovalve that can be triggered by acid or base in aqueous media to release guest molecules entrapped in the nanocontainers of mesoporous organosilica hollow nanospheres (MOHN). The working principle of the nanovalve is illustrated in Figure 1. *N*-Phenylaminomethyltriethoxysilane (PAMTS) was used as the thread molecule, which would functionalize the surface of MOHN. Rhodamine B (RhB) was loaded into the functionalized MOHN as model guest molecules. For the acid-triggered release, β-cyclodextrin (β-CD), not α-CD, was chosen as the capping molecule because β-CD is more hydrophobic and has a larger association constant of complexation with an anilinomethyl group (from PAMTS) in neutral media than α-CD.[15] The addition of acid in the solution would result in the protonation of anilinomethyl group and cause the dissociation of β-CD due to the weakened binding force between β-CD and the anilinomethyl group, leading to the release of RhB. For the base-triggered release, DB24C8 or CB[6] was used as the capping molecule because DB24C8 or CB[6] is able to assemble with dialkylammonium cation (PAMTS) by hydrogen-bonding or ion–dipole interactions in acidic media. Upon deprotonation of dialkylammonium cation by the addition of base, the noncovalent interaction is disrupted and DB24C8 or CB[6] can be dissociated, allowing the loaded RhB to release.

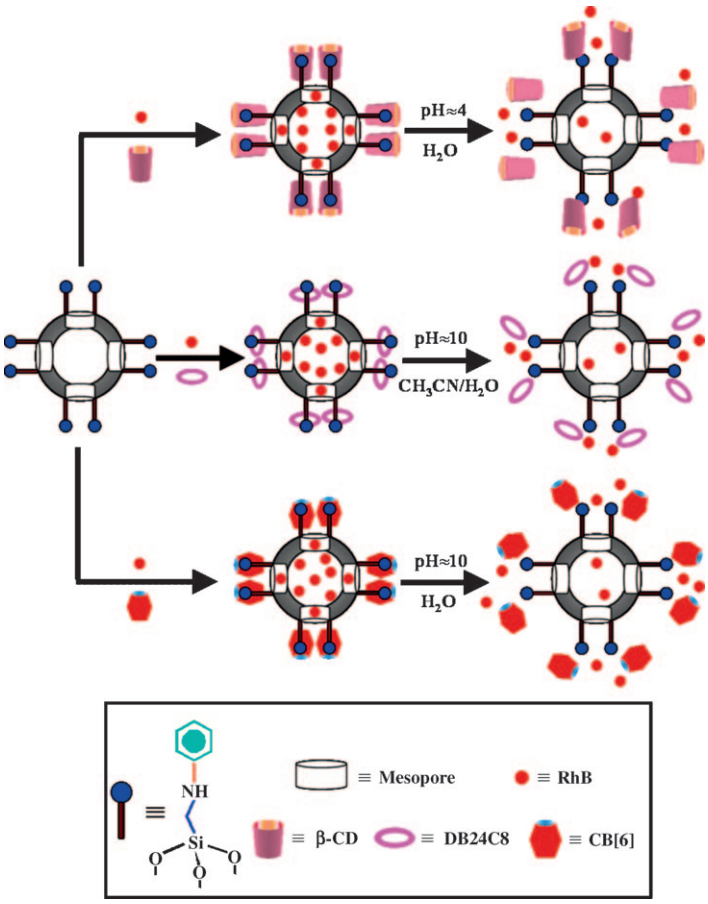

Figure 1. Schematic illustration of pH-responsive, controlled release of rhodamine B (RhB) from nanocontainers of MOHN.

We prepared monodisperse MOHN by using polystyrene (PS) latex spheres as the hard core template. To the best of our knowledge, it is the first time the preparation of individual dispersed PMO hollow nanospheres with uniform particle sizes has been reported. The monodisperse PS spheres were prepared by emulsion polymerization,[16] which has an approximate diameter of (150±10) nm as determined by SEM (Figure S1 in the Supporting Information). The MOHN sample was then synthesized by using cetyltrimethylammonium bromide (CTAB) surfactant and PS latex as the cotemplate, 1,2-bis(trimethoxysilyl)ethane (BTME) as the organosilica source through an NH_4OH-catalyzed sol–gel process. The CTAB mesoporous template was removed by HCl/ethanol solvent extraction and the PS core template was dissolved in THF at room temperature. Figure 2 shows a graphical representation of the synthetic procedure of MOHN. The structure of solvent-extracted MOHN was confirmed by X-ray diffraction (XRD), N_2 adsorption, SEM, dynamic light scattering (DLS), and TEM. As revealed in Figure 3 and Figure S2 in the Supporting Information, the as-synthesized and solvent-extracted samples exhibited a very strong diffraction peak at around 2.1°, typical of short-range ordered mesoporous phase. The N_2 adsorption–desorption isotherm showed a type-IV curve with a well-defined capillary condensation at a relative pressure of 0.2–0.4, thus demonstrating the existence of uniform mesopores. The structural parameters summarized in Table S1 in the Supporting Information displayed a BET surface area of 956 $m^2 g^{-1}$ and a pore size of 2.42 nm for the template-removed sample. Figure 4a shows the SEM image of solvent-extracted MOHN, which was composed of highly uniform particles of (240±10) nm. The narrow particle size distribution was also corroborated by DLS results (polydispersity factor <0.02, see Figure 4c). Furthermore, TEM images (Figure 5a and b) clearly showed a hollow core diameter of (140±10) nm and a mesoporous shell thickness of (50±5) nm for the template-removed MOHN.

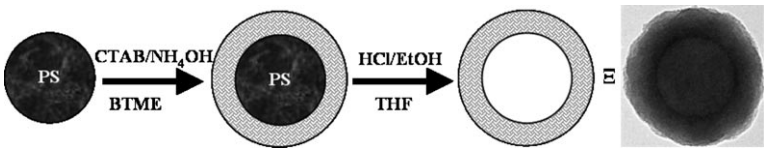

Figure 2. Graphical representation of the preparation of MOHN.

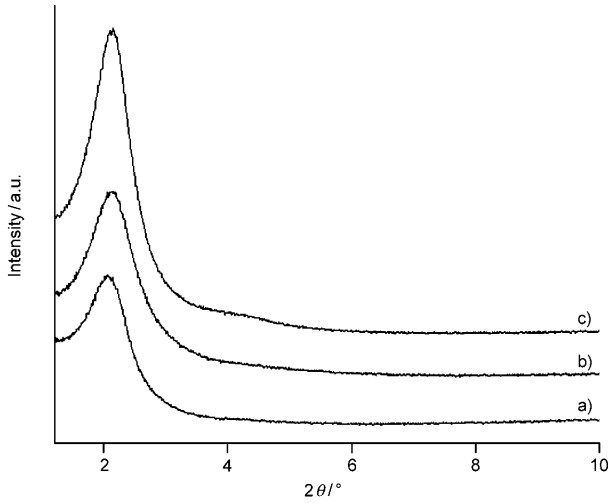

Figure 3. XRD patterns of a) as-synthesized MOHN, b) solvent-extracted MOHN, and c) functionalized MOHN.

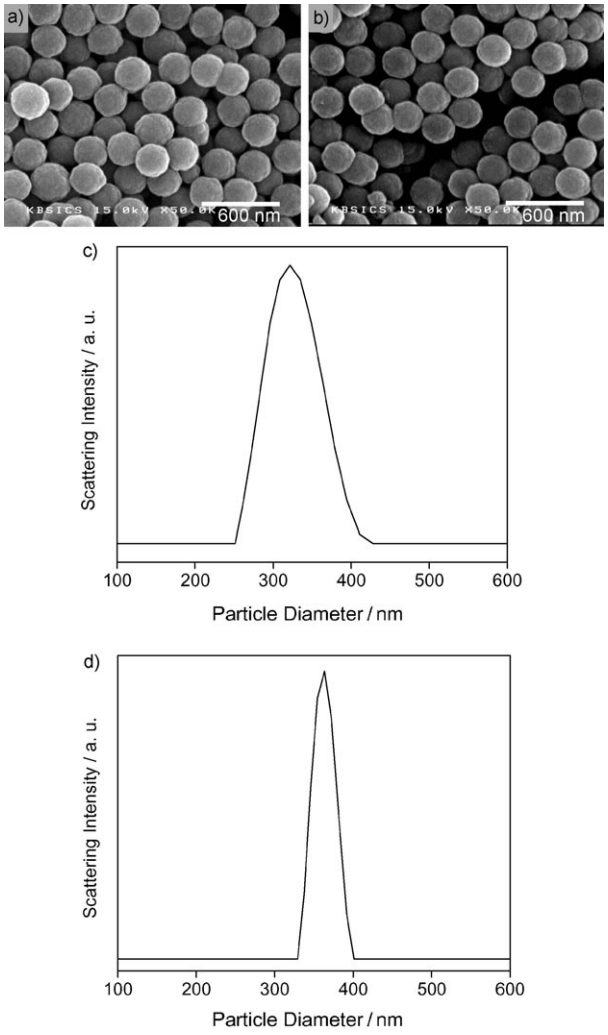

Figure 4. SEM images of a) solvent-extracted MOHN and b) RhB-loaded MOHN. Particle size distributions of c) solvent-extracted MOHN and d) RhB-loaded MOHN.

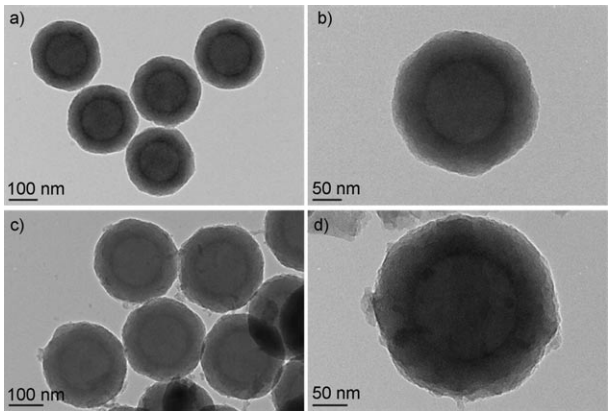

Figure 5. TEM images of a, b) solvent-extracted MOHN and c, d) RhB-loaded MOHN.

Prior to loading of guest molecules, the surface of template-removed MOHN was functionalized with anilinomethyl group. The functionalized MOHN was obtained by heating at reflux the solvent-extracted sample and PAMTS in the presence of anhydrous toluene for 20 h under N_2. The XRD pattern (Figure 3c) exhibited a much stronger diffraction peak in the low 2θ region, suggesting the high structural stability of the MOHN sample. As shown in Figure S2b and Table S1 in the Supporting Information, the functionalized MOHN has a BET surface area of $628\ m^2 g^{-1}$ and a pore size of 2.03 nm, indicating the incorporation of PAMTS on the surface of MOHN. The incorporation of PAMTS was also evidenced by the result of solid-state NMR spectroscopy experiments (Figure S3 in the Supporting Information). The ^{13}C CP MAS NMR spectrum of functionalized MOHN showed one signal in the aliphatic region from the methylene carbon atoms and four benzyl signals in the aromatic region, in addition to the strongest resonance at $\delta = 5.1$ ppm that was attributed to ethane carbon atoms ($-CH_2CH_2-$) in the organosilica framework.[17] The ^{29}Si MAS NMR spectrum of the solvent-extracted MOHN exhibited two signals at $\delta = -57.8$ and -64.4 ppm corresponding to T^2 [RSi-$(OSi)_2OH$] and T^3 [$RSi(OSi)_3$] resonances, respectively. Similarly, one signal at $\delta = -58.3$ ppm was assigned to T^2 resonance and the other signal at $\delta = -63.9$ ppm corresponding to T^3 resonance were observed in the ^{29}Si MAS NMR spectrum of the functionalized MOHN. After deconvolution, the T^3/T^2 ratio of the solvent-extracted sample was calculated to be 1.18, whereas the T^3/T^2 ratio of the functionalized sample was found to be 1.69, demonstrating the incorporation of PAMTS on the surface of organosilica framework. The absence of signals due to Q^n [$Si(OSi)_n(OH)_{4-n}$] species between $\delta = -90$ and -120 ppm indicates that all carbon–silicon bonds were intact under the material synthesis conditions used herein.

To investigate the acid-triggered release property in aqueous media, RhB guest molecules were loaded by soaking the functionalized MOHN in an aqueous solution of RhB. After stirring for 24 h at room temperature, the pH of the mixture was then adjusted to approximately 7, followed by

the addition of a β-CD solution to produce β-CD-capped nanovalves. After an additional 72 h stirring, the loaded, capped sample was separated by filtration, washed thoroughly with water and ethanol to remove unloaded RhB, and dried under vacuum. After loading, the particle stability of the RhB-loaded MOHN was examined by SEM. The particle size distribution curve determined by DLS (Figure 4d) clearly showed that no particle aggregation was observed in the process of loading and capping, indicating the high morphological stability of the MOHN sample. More interestingly, from the TEM images (Figure 5c and d), RhB was directly visualized inside the mesopore of the shell and the hollow core, which was further confirmed by confocal images shown in Figure S4 in the Supporting Information. For the acid-triggered release, the RhB-loaded, β-CD-capped MOHN sample was dispersed in deionized water. The absorbance intensity of RhB in solution was monitored at 556 nm over time. As shown in Figure 6a, at pH≈7, no leakage of the entrapped molecules was observed, revealing the high efficiency of the nanovalve system. After adjusting to pH≈4 by the addition of a 0.2 M aqueous solution of HCl, a steep increase in release percent (absorbance intensity) was observed, indicating the rapid escape of RhB from the nanocontainers of MOHN owing to the dissociation of capping molecule β-CD from the protonated anilinomethyl linker in the mesopore.

DB24C8 was first chosen as the capping molecule to study the base-triggered release property. However, DB24C8 was insoluble in water but soluble in acetonitrile,[18] thus we used CH_3CN and H_2O as the cosolvent. The functionalized MOHN was stirred in an aqueous solution of RhB for 24 h before a solution of DB24C8 in CH_3CN/H_2O cosolvent was added. After stirring for 72 h at room temperature, the RhB-loaded, DB24C8-capped sample was separated and dried under vacuum, followed by dispersion in the CH_3CN/H_2O cosolvent to conduct the controlled release experiment. The release profile was obtained by plotting the absorbance intensity of RhB in solution at 553 nm as a function of time. The DB24C8-capped nanovalve would be activated when a 0.2 M aqueous solution of NaOH was added to adjust the pH of the solution to around 10. At pH≈7, the leakage of RhB was negligible, as indicated from the flat baseline in Figure 6b. At pH≈10, however, the fast release of the loaded RhB was observed owing to the dethreading of DB24C8 from the anilinomethyl linker in the nanovalve system.

Taking the biological application into account, a good nanovalve should be operable in aqueous media without any organic solvent. CB[6] was thus selected as the capping molecule to investigate the base-trigged release property in aqueous media because CB[6] was able to dissolve in acidic solution.[19] The loading, capping, and release experiments were conducted by using the same procedure as that used for the DB24C8-capped system with the same amount of CB[6] (instead of DB24C8) and the same amount of H_2O (instead of CH_3CN) used. Figure 6c shows that the entrapped RhB remained within the nanocontainers of the CB[6]-capped MOHN very well under the neutral aqueous media (pH≈7). Upon adjusting the pH of the solution to pH≈10, a sharp increase in the release percent (absorbance intensity) was observed, indicating the rapid release of RhB from the unblocked mesopores.

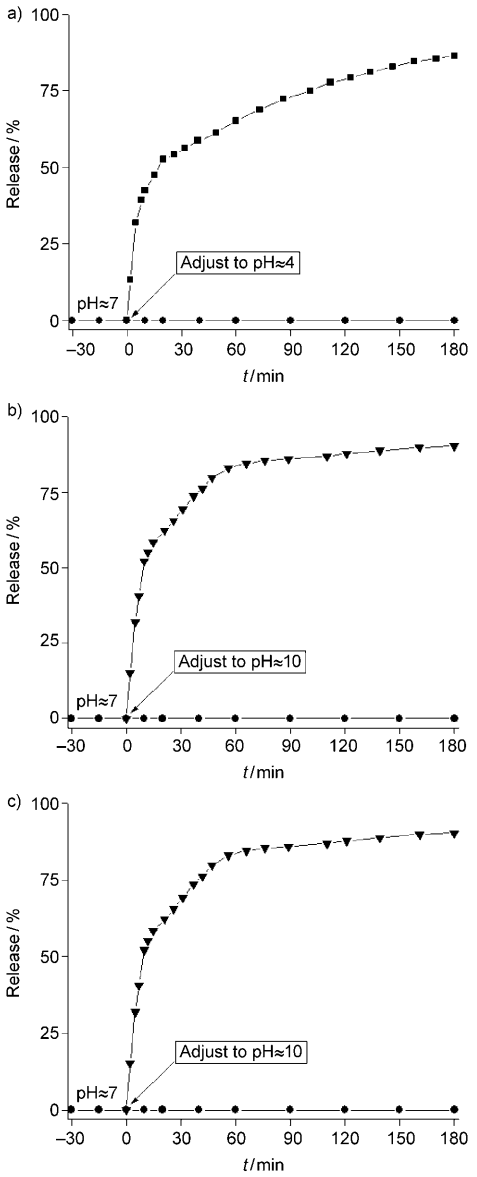

Figure 6. Release profiles of RhB from MOHN capped with a) β-CD, b) DB24C8, and c) CB[6].

In summary, we have demonstrated a general pH-responsive supramolecular nanovalve constructed from mesoporous organosilica hollow nanospheres. The nanovalve is able to operate in aqueous media, contain guest molecules within the hollow core and mesopore shell, and release them by acid/base triggering due to the capping molecule. This is a successful example of a supramolecular nanovalve based on PMO nanoparticles in the form of uniform and monodisperse hollow nanospheres with high structural and morphological stability. Moreover, we have presented a well-de-

signed nanovalve system that can be alternatively trigged by acid or base for the controlled release of the same kind of entrapped guest molecules. The current nanovalve with such unique properties is very promising for the development of smart molecular devices in biosensor and drug delivery applications. For such promising applications of our organosilica-based nanovalve system, detailed studies on the structural stability are now underway.

Experimental Section

Materials: Polyvinylpyrrolidone (PVP-40, Aldrich), potassium persulfate (KPS, Aldrich), styrene (Aldrich), CTAB (Aldrich), ammonia solution (28 wt%, Junsei), BTME (Aldrich), ethyl alcohol (anhydrous, CarloErba), hydrochloric acid (36 wt% HCl, Duksan), tetrahydrofuran (Junsei), acetone (Junsei), toluene (anhydrous, Aldrich), sodium hydroxide (Kanto), PAMTS (Gelest), methyl alcohol (CarloErba), RhB (Aldrich), β-CD (TCI), DB24C8 (Aldrich), acetonitrile (CH_3CN, Junsei), cucurbit[6]uril hydrate (Aldrich). All above chemical reagents were used as received.

Characterization: XRD patterns were recorded on a Rigaku Miniflex diffractometer using $Cu_{K\alpha}$ radiation. Nitrogen adsorption–desorption isotherms were measured at liquid nitrogen temperature using a Micromeritics ASAP 2010 system. SEM images were obtained on a Hitachi S-4200 field emission scanning microscope. Particle size distribution curves were acquired by DLS in ethanol using an Ozuka Electirc/ELS8000 instrument. TEM experiments were performed on a JEOL JEM-2010 electron microscope with an acceleration voltage of 200 kV. ^{29}Si and ^{13}C CP MAS NMR spectra were obtained on a Bruker DSX400 spectrometer at a ^{29}Si resonance frequency of 79.5 MHz and a ^{13}C resonance frequency of 100.6 MHz with tetramethylsilane as the reference. UV/Vis spectra were measured by using a Hitachi U-2010 spectrophotometer. Confocal laser scanning microscope images were taken by using a Zeiss LSM 510 confocal microscope.

Synthesis of polystyrene (PS) latex spheres: The monodisperse PS spheres were prepared by emulsion polymerization initiated by KPS as follows: PVP (1.5 g), KPS (0.20 g), and H_2O (100 g) were loaded into a 250 mL three-bottle flask and stirred at room temperature until dissolution before adding styrene (10 g). The mixture was then deoxygenated by bubbling nitrogen gas for about 1 h. Subsequently the polymerization reaction was carried out at 75 °C for 10 h under a mechanical stirring rate of 100 rpm.

Synthesis of MOHN: CTAB (1.6 g) was dissolved in H_2O (293 g) prior to the addition of a 5.6 wt% PS (12.6 g) solution, ethanol (100 mL), and a 28 wt% ammonia (0.25 g) solution. The resultant mixture was stirred at room temperature for 1 h before the addition of BTME (5.25 g). The above reaction mixture was continuously stirred for an additional 72 h. The solid product was separated by centrifugation, washed with ethanol, and dried under vacuum overnight. The CTAB surfactant and PS template were removed by stirring as-synthesized sample (1.0 g) in ethanol (150 mL) with a 36 wt% aqueous solution of HCl (3.8 g) at 50 °C for 6 h, followed by stirring in THF (100 mL) at room temperature for 12 h. The resulting solid was recovered by centrifugation, washed with THF and acetone several times, and dried at 60 °C under vacuum. To remove CTAB and PS completely, this solvent-extraction procedure was conducted twice.

Functionalization of MOHN with PAMTS: Solvent-extracted MOHN sample (0.5 g) was dispersed in dried toluene (50 mL). PAMTS (0.135 g) was then added to the above mixture, followed by heating at reflux for 20 h under N_2. The functionalized MOHN was obtained by centrifugation, washed with toluene and methanol, and dried at 60 °C under vacuum overnight.

Loading, capping, and release experiments: For β-CD-capped system, RhB (0.048 g) was dissolved in H_2O (10 g) and functionalized MOHN sample (50 mg) was added to the RhB solution followed by sonicating for 15 min and stirring at room temperature for 24 h. The pH of the mixture was then adjusted to about 7. Subsequently, β-CD (0.11 g) was dissolved in H_2O (4 g) and the β-CD solution was added dropwise to the pH-adjusted mixture. After sonicating for 15 min, the resultant mixture was stirred for 3 d. The loaded, capped sample was obtained by filtration through a 0.2 μm porous membrane, washed thoroughly with water and ethanol, and dried at room temperature under vacuum. To investigate the pH-responsive property, the RhB-loaded, β-CD capped MOHN sample (8.0 mg) was dispersed in deionized water (8 g). Release profiles were recorded by plotting the absorbance intensity of RhB in solution at 556 nm as a function of time. The β-CD-capped nanovalve was activated upon adjusting the pH of the solution to around 4 by adding a 0.2 M aqueous solution of HCl. For the DB24C8-capped system, after sonicating for 15 min and stirring for 24 h at room temperature, the mixture with PAMTS-functionalized MOHN (50 mg), RhB (0.048 g), H_2O (10 g) was added to a solution of DB24C8 (44.8 mg) in CH_3CN (4 g), followed by stirring for 3 d at room temperature. After the same separation treatment as mentioned above, the RhB-loaded, DB24C8-capped sample (8.0 mg) was dispersed in H_2O (6 g) and CH_3CN (2 g). During the controlled-release experiment, the absorbance intensity of RhB in solution was measured at 553 nm. The DB24C8-capped nanovalve was activated upon adjusting the pH of the solution to around 10 by the addition of a 0.2 M aqueous solution of NaOH. For the CB[6]-capped system, the procedure for the loading, capping, and release experiment was the same as that used for the DB24C8-capped system with the same amount of CB[6] (instead of DB24C8) and H_2O (instead of CH_3CN).

Acknowledgements

The work was supported by the National Research Foundation of Korea (NRF) grant funded by the Ministry of Education, Science and Technology, Korea (MEST) (Acceleration Research Program (no. 2009-0078791; Pioneer Research Center Program), the Korea–China Joint Research Center Program (K20807000001-09B1200-00110) of NRF, a grant from the Fundamental R&D Program for Core Technology of Materials funded by the Ministry of Knowledge Economy, Korea, and the Brain Korea 21 Project of the MEST.

Keywords: delivery systems · mesoporous materials · pH responsive · rotaxanes · supramolecular chemistry

[1] a) S. Angelos, E. Johansson, J. F. Stoddart, J. I. Zink, *Adv. Funct. Mater.* **2007**, *17*, 2261; b) B. G. Trewyn, I. I. Slowing, S. Giri, H.-T. Chen, V. S.-Y. Lin, *Acc. Chem. Res.* **2007**, *40*, 846; c) S. Angelos, M. Liong, E. Choi, J. I. Zink, *Chem. Eng. J.* **2008**, *137*, 4; d) M. Liong, S. Angelos, E. Choi, K. Patel, J. F. Stoddart, J. I. Zink, *J. Mater. Chem.* **2009**, *19*, 6251.

[2] a) A. B. Descalzo, R. Martínez-Máñez, F. Sancenón, K. Hoffmann, K. Rurack, *Angew. Chem.* **2006**, *118*, 6068; *Angew. Chem. Int. Ed.* **2006**, *45*, 5924; b) V. Balzani, A. Credi, M. Venturi, *ChemPhysChem* **2008**, *9*, 202; c) S. Silvi, M. Venturi, A. Credi, *J. Mater. Chem.* **2009**, *19*, 2279.

[3] S. Saha, K. C.-F. Leung, T. D. Nguyen, J. F. Stoddart, J. I. Zink, *Adv. Funct. Mater.* **2007**, *17*, 685.

[4] a) R. Hernandez, H.-R. Tseng, J. W. Wong, J. F. Stoddart, J. I. Zink, *J. Am. Chem. Soc.* **2004**, *126*, 3370; b) T. D. Nguyen, H.-R. Tseng, P. C. Celestre, A. H. Flood, Y. Liu, J. F. Stoddart, J. I. Zink, *Proc. Natl. Acad. Sci. USA* **2005**, *102*, 10029; c) T. D. Nguyen, Y. Liu, S. Saha, K. C.-F. Leung, J. F. Stoddart, J. I. Zink, *J. Am. Chem. Soc.* **2007**, *129*, 626; d) R. Liu, X. Zhao, T. Wu, P. Feng, *J. Am. Chem. Soc.* **2008**, *130*, 14418.

[5] a) T. D. Nguyen, K. C.-F. Leung, M. Liong, Y. Liu, J. F. Stoddart, J. I. Zink, *Adv. Funct. Mater.* **2007**, *17*, 2101; b) J. Lu, E. Choi, F. Tamanoi, J. I. Zink, *Small* **2008**, *4*, 421; c) D. P. Ferris, Y.-L. Zhao, N. M. Khashab, H. A. Khatib, J. F. Stoddart, J. I. Zink, *J. Am. Chem. Soc.* **2009**, *131*, 1686; d) C. Park, K. Lee, C. Kim, *Angew. Chem.* **2009**, *121*, 1301; *Angew. Chem. Int. Ed.* **2009**, *48*, 1275.
[6] a) K. Patel, S. Angelos, W. R. Dichtel, A. Coskun, Y.-W. Yang, J. I. Zink, J. F. Stoddart, *J. Am. Chem. Soc.* **2008**, *130*, 2382; b) A. Schlossbauer, J. Kecht, T. Bein, *Angew. Chem.* **2009**, *121*, 3138; *Angew. Chem. Int. Ed.* **2009**, *48*, 3092; c) A. Bernardos, E. Aznar, M. D. Marcos, R. Martínez-Máñez, F. Sancenón, J. Soto, J. M. Barat, P. Amorós, *Angew. Chem.* **2009**, *121*, 5998; *Angew. Chem. Int. Ed.* **2009**, *48*, 5884; d) C. Park, H. Kim, S. Kim, C. Kim, *J. Am. Chem. Soc.* **2009**, *131*, 16614.
[7] K. C.-F. Leung, T. D. Nguyen, J. F. Stoddart, J. I. Zink, *Chem. Mater.* **2006**, *18*, 5919.
[8] T. D. Nguyen, K. C.-F. Leung, M. Liong, C. D. Pentecost, J. F. Stoddart, J. I. Zink, *Org. Lett.* **2006**, *8*, 3363.
[9] S. Angelos, Y.-W. Yang, K. Patel, J. F. Stoddart, J. I. Zink, *Angew. Chem.* **2008**, *120*, 2254; *Angew. Chem. Int. Ed.* **2008**, *47*, 2222.
[10] C. Park, K. Oh, S. C. Lee, C. Kim, *Angew. Chem.* **2007**, *119*, 1477; *Angew. Chem. Int. Ed.* **2007**, *46*, 1455.
[11] L. Du, S. Liao, H. A. Khatib, J. F. Stoddart, J. I. Zink, *J. Am. Chem. Soc.* **2009**, *131*, 15136.
[12] a) M. V. Landau, S. P. Varkey, M. Herskowitz, O. Regev, S. Pevzner, T. Sen, Z. Luz, *Microporous Mesoporous Mater.* **1999**, *33*, 149; b) M. C. R. Hernández, J. E. M. Wejebe, J. I. V. Alcántara, R. M. Ruvalcaba, L. A. G. Serrano, J. T. Ferrara, *Microporous Mesoporous Mater.* **2005**, *80*, 25.
[13] a) S. Inagaki, S. Guan, Y. Fukushima, T. Ohsuna, O. Terasaki, *J. Am. Chem. Soc.* **1999**, *121*, 9611; b) W. Guo, X. S. Zhao, *Microporous Mesoporous Mater.* **2005**, *85*, 32; c) S. Hudson, J. Cooney, B. K. Hodnett, E. Magner, *Chem. Mater.* **2007**, *19*, 2049.
[14] a) M. Park, S. S. Park, M. Selvaraj, D. Zhao, C.-S. Ha, *Microporous Mesoporous Mater.* **2009**, *124*, 76; b) W. Cai, I. R. Gentle, G. Q. Lu, J.-J. Zhu, A. Yu, *Anal. Chem.* **2008**, *80*, 5401.
[15] L. Liu, Q.-X. Guo, *J. Phys. Chem. B* **1999**, *103*, 3461.
[16] H. Zou, S. Wu, Q. Ran, J. Shen, *J. Phys. Chem. C* **2008**, *112*, 11623.
[17] W. Guo, J.-Y. Park, M.-O. Oh, H.-W. Jeong, W.-J. Cho, I. Kim, C.-S. Ha, *Chem. Mater.* **2003**, *15*, 2295.
[18] Y. Takeda, *Bull. Chem. Soc. Jpn.* **1983**, *56*, 3600.
[19] K. Kim, N. Selvapalam, Y. H. Ko, K. M. Park, D. Kim, J. Kim, *Chem. Soc. Rev.* **2007**, *36*, 267.

Received: April 16, 2010
Published online: June 30, 2010

